17th World Conference on Earthquake Engineering, 17WCEE
Sendai, Japan - September 13th to 18th 2020

EXPERIMENT ON SMRF CONSIDERING MULTIPLE EARTHQUAKES PART 1 THE TEST SPECIMEN & LOADING PROTOCOL

R. Tenderan[(1)], K. Kohtaki[(2)], T. Isihda[(3)], S. Yamada[(4)], S. Kishiki[(5)], T. Seike[(6)], T. Hasegawa[(7)], J. Iyama[(8)], S. Yagi[(9)], N. Tatsumi[(10)]

[(1)] *Graduate student, Tokyo Institute of Technology, tenderan.r.aa@m.titech.ac.jp*
[(2)] *Graduate student, Tokyo Institute of Technology, kotaki.k.aa@m.titech.ac.jp*
[(3)] *Assistant Prof., Tokyo Institute of Technology, ishida.t.ae@m.titech.ac.jp*
[(4)] *Associate Prof., Tokyo Institute of Technology, kishiki.s.aa@m.titech.ac.jp*
[(5)] *Prof., Tokyo Institute of Technology, yamada.s.ad@m.titech.ac.jp*
[(6)] *Prof., The University of Tokyo, seike@edu.k.u-tokyo.ac.jp*
[(7)] *Chief Researcher, Building Research Institute, hase@kenken.go.jp*
[(8)] *Associate Prof., The University of Tokyo, iyama@arch1.t.u-tokyo.ac.jp*
[(9)] *Graduate student, The University of Tokyo, 6952829840@edu.k.u-tokyo.ac.jp*
[(10)] *Assistant Prof., Tokyo Institute of Technology, tatsumi.n.aa@m.titech.ac.jp*

Abstract

The occurrence of multiple strong shocks in a short period of time recently pointed out; for example, in the 2016 Kumamoto Earthquake, two strong shocks struck the area within two days. Those two strong shocks are recorded to have an intensity 7 (JMA intensity scale) in the most damaged area, i.e., Mashiki Town. Within this short period of time, any structural repairs could hardly be done; thus, the structure should be able to sustain multiple strong shocks at once. The current seismic design code ensures that buildings do not collapse against the severe earthquake, which is expected to occur once during the lifetime. However, in case multiple strong earthquakes struck the building continuously, whether the buildings can resist them all or not without collapsing remains unclear. Therefore, this study aims to measure the performance of buildings against multiple earthquakes. The performance of buildings is not limited to the structural performance only but also the nonstructural components; because, even though the structural members are not damaged, the function of a building can not be maintained if the nonstructural components, such as interior or exterior walls, are severely damaged.

In this study, a cyclic-loading test was conducted to a full-scale steel moment-resisting frame (SMRFs) specimen. The SMRF specimen consists of columns in the four corners (height of 3.5 m) and two floor areas (6 m × 2.5 m) at the upper and lower side of the columns. This specimen represents an intermediate story of the middle- or low-rise steel building. The two plane frames in the longer direction (6 m span × 3.5 m height) are the main observed frame in this test; thus, two horizontal jacks were attached at the upper beam level of each plane frame, and a one direction cyclic loading was conducted by giving the same displacement to each plane frame. Two different details of a beam-to-column connection were used in those two plane frames. One plane frame uses the beam-to-column connection type with the weld-access hole, while the other one is without the weld-access hole. Also, the concrete slab was cast on the upper and lower floor area.

In this test, two specimens were used. The structural system of those two specimens are typical, but the nonstructural component attached to the steel frame was different. In the first specimen, the light gauge steel (LGS) partition wall (interior wall type) is installed, while in the second specimen, the autoclaved lightweight concrete (ALC) panel (exterior wall type) is installed to the steel frame. The loading protocol used in this test simulates the occurrence of multiple earthquakes. At first, one set of loading history, which corresponds to one earthquake, was determined from the inelastic time-history response analysis of a 3-story SMRF model under various ground motion records. Then, this set is scaled to various intensity levels; and during the test, multiple sets were performed with the incremental and decremental variations of intensity level to simulates the occurrence of multiple earthquakes.

Keywords: Steel moment-resisting frame; Cyclic loading test; Multiple earthquakes

1. Introduction

In the Japanese seismic code, buildings are designed not to collapse when a building is subjected to a strong earthquake once. However, the occurrence of multiple strong shocks in a short period of time recently pointed out; for example, in the 2016 Kumamoto Earthquake, two strong shocks struck the area within two days [1]. Those two strong shocks are recorded to have an intensity 7 (JMA intensity scale) in the most damaged area, i.e., Mashiki Town. Within this short period of time, any structural repairs could hardly be done; thus, the structure should be able to sustain multiple strong shocks at once. Therefore, this study aims to measure the performance of buildings against multiple earthquakes.

Furthermore, there have been confirmed cases where damage to nonstructural components occurred even though structural components were almost no damage [2]. In addition, it has been confirmed that nonstructural components impart strength to buildings [3]. Therefore, in order to evaluate the seismic performance of whole buildings, it is necessary to consider not only structural components but also nonstructural components. In this study, cyclic loading tests of steel frame with nonstructural components were conducted to evaluate the damage, seismic performance, and functionality of steel building under multiple earthquakes.

2. Specimen

In this experiment, two full-scale steel moment-resisting frame (SMRF) specimens were tested. Fig. 1 shows the setup and geometry of the specimen. The specimen represents a one-story one-span of an intermediate story of the middle- or low-rise steel building. The floor area of the specimen is 6 m × 2.5 m and the height is 3.5 m. In this test, the main focus of the experiment is the steel frames on the NS direction (6 m × 3.5 m); thus, two oil jacks were attached at the top corner of the two steel frames in the NS direction. The oil jacks were connected to the strong wall, while the specimen was connected to the strong floor using the pin joint at the four corners.

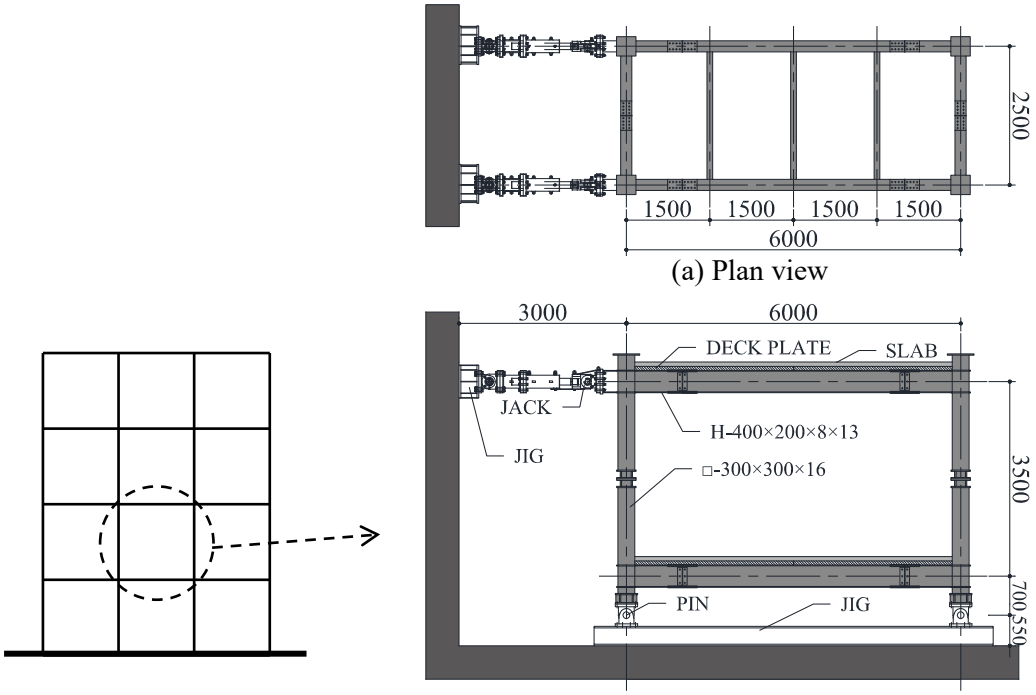

(a) Plan view

(b) East elevation view

Fig. 1 – Test setup

Table 1 – Cross sections and material properties

Member		Material	Section*	σ_y[N/mm^2]	σ_u[N/mm^2]
Column		BCR295	□-300×16	363.3	402.2
Beam	Flange	SN400B	H-400×200×8×13	276.6	409.5
	Web			377.3	458.1
Member		Material	Specimen	σ_c[N/mm2]	σ_t[N/mm2]
Slab		f_c' 20 Mpa	1st (LGS frame)	41.7	3.2
			2nd (ALC frame)	27.8	2.5

* □ - width × thickness; H - depth × width × web thickness × flange thickness
* σ_y : yield strength of steel; σ_u : tensile strength of steel
* σ_c : compression strength of concrete; σ_t : tensile strength of concrete

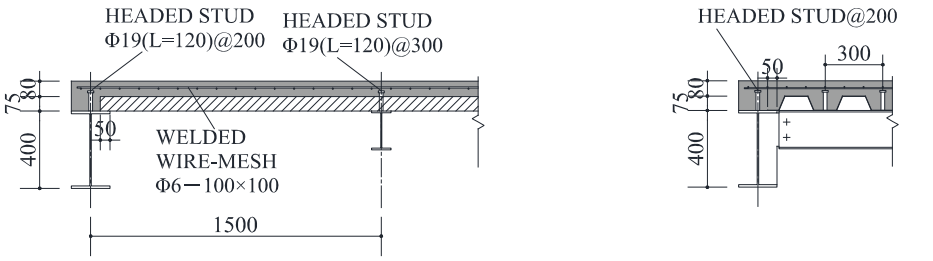

(a) Long side direction (b) Short side direction

Fig. 2 – Outline of the slab

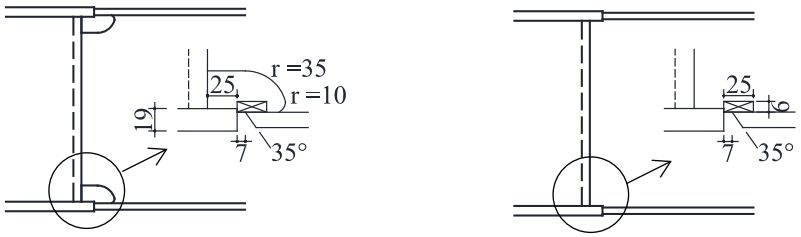

(a) With weld-access hole, E-plane (b) Without weld-access hole, W-plane

Fig. 3 – Beam end connection type of each plane

Both of the specimens have almost the same detail of structural components. The column members use the square hollow section (SHS) with material type of BCR295 (nominal yield strength = 295 N/mm^2; nominal tensile strength = 400 N/mm^2), while the beam members use the wide flange section with material type of SN400B (nominal yield strength = 235 N/mm^2; nominal tensile strength = 400 N/mm^2). The cross-sections and actual material properties (obtained from the material test) are shown in Table 1. The section of beams and columns were designed by considering the ratio of the nominal yield moment of the column to the nominal full plastic moment of the beam is more than or equal to 1.5 to ensure that the strong-column weak-beam mechanism can be reliably formed.

In the EW direction, in addition to the main beam, secondary beams (H-200×100×5.5×8) were attached every 1.5 m to provide lateral support to the main beams in NS direction (Fig. 1(a)). At the upper and lower floor, reinforced concrete slabs (thickness of 80 mm) were cast on the deck plate (height of 75 mm) as shown in Fig. 2. The slabs were connected to the steel beam by the shear stud. The spacing of the shear stud was

determined according to Design Recommendations for Composite Constructions to create full composite action between the steel beam and the concrete slab [4].

As shown in Fig. 1, within one specimen, there are two typical steel frames in the NS direction, i.e., E-plane and W-plane (Fig. 1(a)). The main difference between these two steel frames is the detail of the beam-to-column connection. Two typical type of details which are commonly employed in Japan are used in this experiment. As shown in Fig. 3, the beam end connections of E-plane have a weld access hole that conforms to JASS 6, while those of W-plane have no weld access hole [5]. These two types of beam-to-column connection detail are the new enhanced type of details which have been improved after the 1995 Kobe earthquake to prevent the early fracture and stress concentration at the toe of the weld access hole. In both types of connection, the wide-flange section beams were shop-welded to the SHS column through the diaphragms.

While the structural component of both specimens is the same, the nonstructural component attached to the 1st and 2nd specimens is different. For the 1st specimen, the light gauge steel (LGS) partition wall type, which is one of the types of an interior wall, was installed to the steel frames. The LGS partition wall mainly composes of two layers of gypsum board and the light gauge steel (LGS) foundation frame to support the boards. Meanwhile, in the 2nd specimen, the autoclaved lightweight concrete (ALC) wall type, which is one of the types of an exterior wall, was attached to the steel frames. The ALC wall was attached in the outside of the steel frame with a vertical rocking installation system and mainly composes of the autoclaved lightweight concrete (ALC) panel and supporting angles that were attached around door and window openings to support the panels. Hereafter, the 1st and 2nd specimens will be referred to as “LGS frame” and “ALC frame”, respectively.

Fig. 4 shows the photos of each plane of the LGS frame, while Fig. 5 shows the plan view of the LGS wall. As shown in both figures, the configuration of the LGS wall in the E-plane and W-plane is different. In the E-plane, all of the partition walls were installed aligned with the steel frame (flat part). Meanwhile, in the W-plane, some part of the partition wall was not installed aligned with the steel frame (eccentric part), and adoor opening is provided in the partition wall (opening part). These three types of configuration are considered to be commonly used for the interior partition wall in the real buildings.

Fig. 6 shows the photos of each plane of the ALC frame, while Fig. 7 shows the elevation view of the ALC wall. Similar to the LGS frame, the configuration of the ALC wall is designed to be different in both planes to consider some typical configurations for the exterior wall type. As shown in the figures, the E-plane’s wall has no openings, while the W-plane’s wall has two openings for a door and a window.

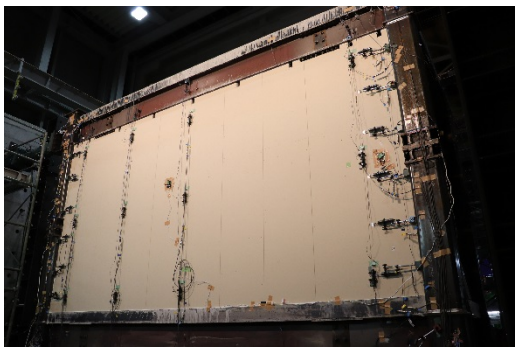

(a) E-plane

(b) W-plane

Fig. 4 – LGS frame

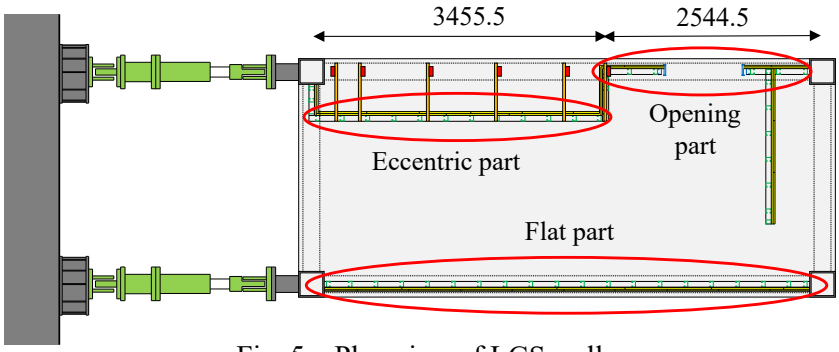

Fig. 5 – Plan view of LGS wall

(a) E-plane (b) W-plane

Fig. 6 – ALC frame

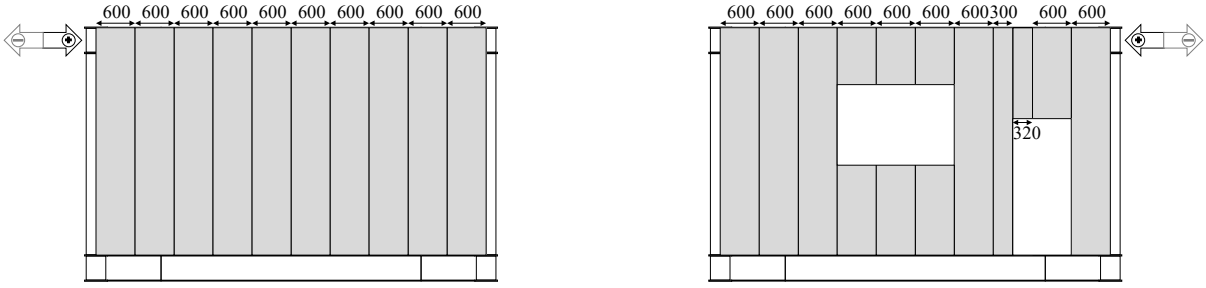

(a) E-plane (b) W-plane

Fig. 7 – Elevation view of ALC wall

3. Loading Protocol

As explained in the previous section, two oil jacks were attached at the top corner of the E-plane and W-plane. During the loading, the static lateral force was generated from the jacks to the specimen in the NS direction. The loading was controlled by the lateral displacement of the frames, and the same displacement was given to both planes at the same time. In this test, the jack push direction is defined as positive loading and jack pull direction is defined as negative loading.

To simulate the occurrence of multiple earthquakes, a special type of loading history was created from an inelastic time history response analysis result. The 3-story model of SMRF used by Tenderan et al. [6] to evaluate the seismic performance of SMRF under multiple strong earthquakes was adopted for the time history

response analysis. Ten different input ground motions were used in the analysis as listed in Table 2. All of the ground motions were scaled to the intensity of peak ground velocity = 0.5 m/s to standardize the intensity.

From the response analysis, the story drift angle (R) time history response at the 2nd story was extracted, and the rainflow counting algorithm [7] was performed to obtain the number of cycles of each amplitude. Then, each amplitude in each case was grouped into five groups based on the ratio to its maximum amplitude (R_{max}). Table 2 shows the number of cycles in each group for each case of input ground motion. The average values shown in Table 2 were calculated after excluding the maximum and minimum value in each group. Then, one set of loading history was created according to the average values shown in Table 2; thus one set of loading history consists of 0.4 R_{max} × 4 cycles, 0.6 R_{max} × 2 cycles, 0.8 R_{max} × 2 cycles, 1.0 R_{max} × 1 cycle. Noting that the group of 0.1~0.3 R_{max} was neglected and the number of cycles of group 0.3~0.5 R_{max} was reduced to half because the effect of these small-amplitude loadings to the specimen was assumed to be negligible, and also because of the time constraint in conducting the experiment. The typical one set of loading history is shown in Fig. 8. The cycles were symmetrically arranged by positioning the maximum amplitude cycle at the center. This one set of loading history is considered to correspond to one earthquake.

During the test, multiple sets of loadings were performed with the incremental and decremental variations of maximum amplitude (R_{max}) to simulate the occurrence of multiple earthquakes. The magnitude of the loading set was adjusted by adjusting the R_{max}. Fig. 9 shows the variation of R_{max}. In total, nine sets of loading

Table 2 – Number of cycles of each group

No.	Earthquake	0.1~0.3 R_{max}	0.3~0.5 R_{max}	0.5~0.7 R_{max}	0.7~0.9 R_{max}	0.9~1.0 R_{max}
1	El Centro	35	8	5	2	1
2	Taft	31	11	6	4	1
3	Hachinohe	65	8	2	3	1
4	Gilroy Array #3	27	12	1	2	2
5	Newhall	13	4	0	1	1
6	Olive View	12	1	2	1	1
7	JMA Kobe	16	9	1	1	1
8	TCU129	28	7	3	1	1
9	JMA Sendai	101	45	4	2	1
10	Kik-net Mashiki	12	2	1	0	1
	Average	**28**	**8**	**2**	**2**	**1**

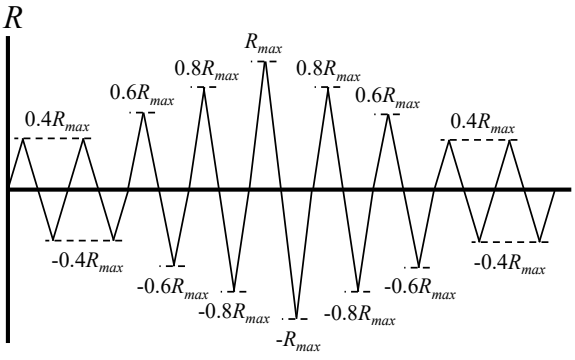

Fig. 8 – Typical one set of loading history

Set No.	R_{max}
1	1/400
2	1/200
3	1/100
4	1/200
5	1/75
6	1/100
7	1/50
8	1/75
9	1/33

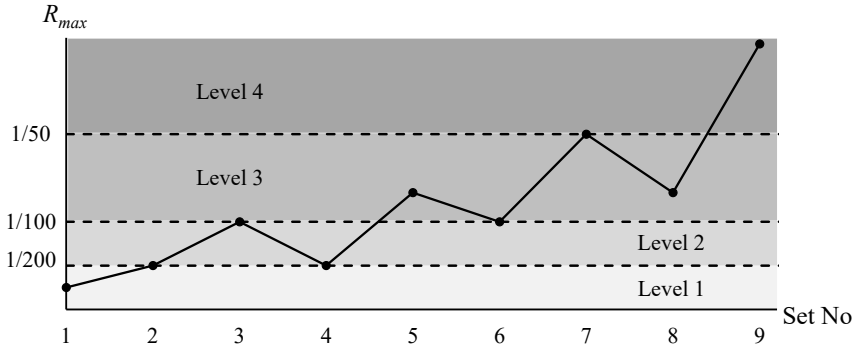

Fig. 9 – Maximum SDA of each set and the corresponding earthquake level

were planned to be conducted for each specimen. The loading sets can be grouped into four different groups based on the R_{max}; each level corresponds to an earthquake with a certain intensity. Level 1 is the lowest level with the limitation of R_{max} of 1/200; in this level, the structure is expected to remain in the elastic range. For the level 2, the limitation of R_{max} is taken to be twice of level 1 since 1/100 is commonly used as the targeted maximum story drift angle (SDA) in the design to guarantee the performance of SMRF and a certain type of nonstructural components, such as ALC wall. The next two levels, level 3 and 4, are considered to be the over-design level; for level 3, the limitation of R_{max} is taken to be twice of level 2 (1/50), while level 4 is including all levels with R_{max} above the limitation of level 3.

4. Measurement Plan

The measurement and method to obtain the actual value of SDA and the shear force acting on the specimen are covered in this section. In this test, the SDA is defined as the ratio of the relative horizontal displacement of the centerline of the upper and lower beams to the story height which is the vertical distance between the centerline of the upper and lower beams. The SDA is obtained from the measured displacement at each node (δ). Fig. 10 shows the position of displacement transducers. δ is obtained by averaging the two displacement transducers that measure the absolute displacement at the upper and lower diaphragms. Then, the SDA (R) is calculated by the equation shown in Fig. 12. In this test, deformation and shear force in positive loading are expressed with the positive sign, and those in negative loading is expressed with the negative sign.

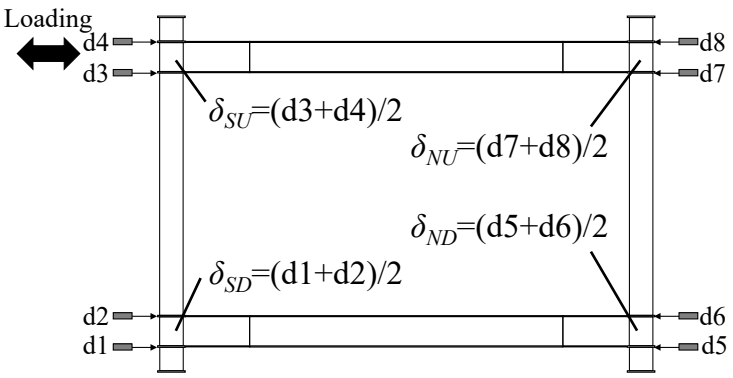

Fig. 10 – Position of displacement transducers to obtain δ

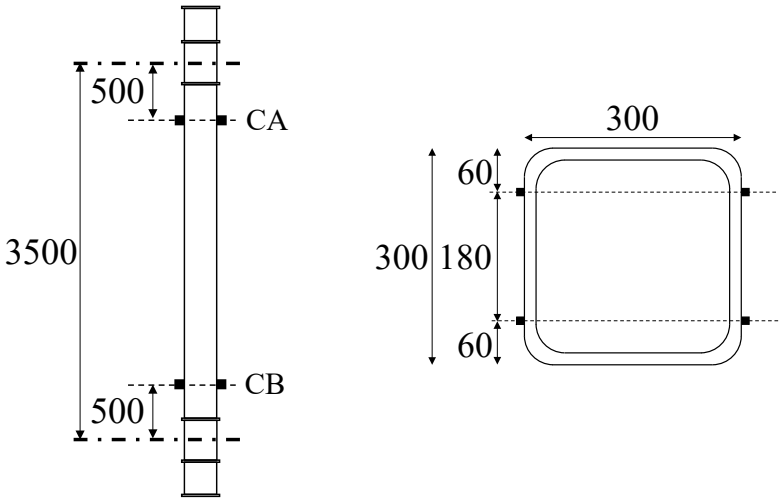

(a) Attached section (b) Attached position

Fig. 11 – Position of strain gauges to obtain ${}_cQ$

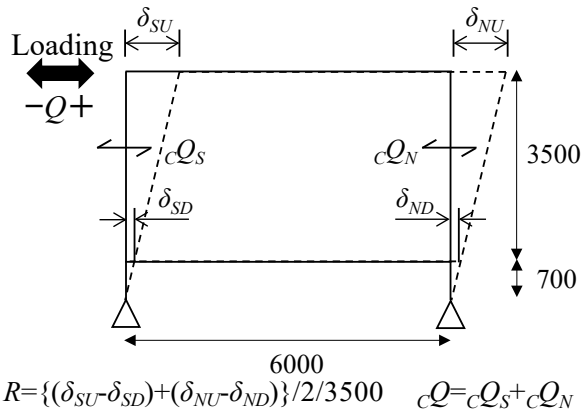

Fig. 12 – Calculation method to obtain R and ${}_cQ$

To measure the shear force acting on the steel frames (${}_cQ$), strain gauges were attached to the columns. Fig.11 shows the attached position of the strain gauges. The strain gauges were attached at two sections per column which are called the CA and CB section, and four strain gauges were attached per section in the column flanges. Then, the bending moment acting on the section CA and CB (M_{CA} and M_{CB}) were calculated using the measured strain assuming plain section remains plain and bilinear relation stress-strain curve. By assuming the linear moment distribution along the column, the shear force acting on the column can be obtained by dividing the sum of M_{CA} and M_{CB} by the distance between the CA and CB section. Then, ${}_cQ$ can be obtained by summing the shear force acting on both columns as shown in Fig. 12. Lastly, the shear force acting on the nonstructural component can be calculated by subtracting the shear force acting on the whole specimen (Q) and ${}_cQ$; Q was measured by the load cell in the oil jacks in this test.

5. Conclusions

In this paper, the outline of the specimen, loading protocol and measurement plan are reported. Two full-scale SMRF specimens were tested. The specimen represents a one-story one-span of an intermediate story of the middle- or low-rise steel building. The detail of the beam-to-column connection of the two planes in one

specimen was different. The structural component of both specimens is the same; however, the nonstructural component attached to the 1st and 2nd specimens is different. In the 1st specimen, LGS wall (generally used as a partition wall) was attached to the steel frame, and in the 2nd specimen, the ALC wall (generally used as an exterior wall) was attached to the steel frame.

One typical set of loading history that corresponds to one earthquake was created based on the response analysis results. And multiple sets of loading with various levels were conducted to consider the effect of multiple earthquakes. The shear force acting on the whole specimen was measured by the load cell in the oil jacks in this test. Meanwhile, the shear force acting on the steel frame was calculated by the strain of the steel column. Then, the shear force acting on the nonstructural components was calculated by subtracting the shear force acting on the whole specimen by the shear force acting on the steel frame.

Acknowledgement

This work is supported by Japan Society for the Promotion of Science KAKENHI Grant Number JP17H01302. Deck plates were provided by Composite Slab Industrial Association, and driving pins were provided by Max Co. Ltd. Their financial supports are gratefully acknowledged. The authors also thank Dr. Norihito Miki for his support during the preparation of the experiment.

References

[1] Kato A, Nakamura K, and Hiyama Y (2016): The 2016 Kumamoto earthquake sequence. *Proceedings of Japan Academy*, Series B, **92**(8), 358–371.

[2] Iyama J, Matsuo S, Kihsiki S, Ishida T, Azuma K, Kido M, Iwashita T, Sawada K, Yamada S, and Seike T (2018): Outline of reconnaissance of damaged steel school buildings due to the 2016 Kumamoto earthquake. *Journal of Technology and Design (Transactions of AIJ)*, **24**(56), 183-188 (in Japanese).

[3] Matsuoka Y, Suita K, and Nakashima M (2013): Effect of non-structural components for total behavior of steel building: a proposal of hysteretic model for external walls and partition walls. *Proceedings of Structural Engineering. B (AIJ)*, **59B**, 191-199 (in Japanese).

[4] Architectural Institute of Japan (AIJ) (2010): Design recommendations for composite constructions, 3rd edtion (in Japanese).

[5] Architectural Institute of Japan (AIJ) (2018): Japan Architectural Standard Specification JASS 6 Steel Work, 11th edition (in Japanese).

[6] Tenderan R, Ishida T, Jiao Y, and Yamada S (2019): Seismic performance of ductile steel moment-resisting frames subjected to multiple strong ground motions. *Earthquake Spectra*, **35**(1), 289−310.

[7] Endo T, Matsuishi M, Mitsunaga K, Kobayashi K, and Takahashi K (1974): Rainflow method, the proposal and the applications. *Bulletin of Kyushu Institute of Technology*, **28**, 33–26 (in Japanese).

